Seismic Performance of Reinforced Concrete Columns Retrofitted with FRP and Steel Plates

H. Araki & T. Tokunaga
Hiroshima University, Japan

SUMMARY
This paper presents the seismic performance of RC columns jacketed with high strength “polyarylate” fiber sheets, thin steel plates without welding, and grout mortar. Static loading tests were carried out using scaled RC columns to investigate the resistance mechanism of the retrofitted RC columns. Five test columns were subjected to cyclic lateral loads under lateral displacement control. The column section was 300mmx300m, and the shear span was 1260mm. The test columns were designed to replicate existing columns, of which the ratio of the shear strength to the flexural strength was 1:1.12.
The behaviour of the test column without retrofitting was brittle in the load deflection curve, and compression failure in the concrete cover was observed at both ends of the test column. The maximum lateral strength and the ductility in the test columns retrofitted with the proposed method were significantly increased.

Keywords: RC Column, Seismic performance, Jacketing, FRP sheet, Steel plate

1. INTRODUCTION

Various methods of retrofitting existing buildings have been proposed in Japan after the experience of previous earthquake disasters. In order to increase the ductility of the reinforced concrete (RC) columns, jacketing of the steel plates or the FRP (fiber reinforced plastics) sheets were the standard retrofitting method, in order to change from the brittle failure type to the ductile failure type. When using the steel plates, the cost of construction increases due to welding of the steel plates and the necessity of heavy machinery. On the other hand, when using FRP, it is noted that the high tensile strength of the fiber is not properly evaluated due to the bond strength to the concrete and the local strain of the FRP sheet, although the construction performance is very high.
Therefore, a retrofitting method using both the divided steel plates and FRP sheet was proposed (Ito 2007). Taking the divided steel plates together with continuous FRP sheets, the disadvantages of the previous retrofitting methods mentioned above were improved. It is considered that the flexural strength of the retrofitted RC column does not increase because the previous methods usually have clearance at both ends of the column, but it is effective in improving the ductility of the shear failure type RC column. In the proposed method, the clearance is not only constructed in order to increase the flexural strength, but also to improve ductility. The resistance mechanism of increasing flexural strength is discussed in this paper.

1.1. Purpose

This paper presents the seismic performance of RC columns jacketed with high strength polyarylate fiber sheets, thin steel plates without welding and grout mortar. Typically, glass fiber, carbon fiber and aramid fiber are popular FRP materials used in jacketing RC columns. Polyarylate fiber is a new material that has been used in the Space Shuttle as a structural element. The parameters considered in the experiment were the thickness of the thin steel plate, the number of FRP sheets, and wrapping and welding of the steel plate. The effect of each variable was evaluated by the seismic performance.

2. EXPERIMENTAL PROCEDURE

2.1. Test columns

The original test columns were designed as the flexural failure type according to the old RC Standard of the Architectural Institute of Japan. The list of test columns is shown in Table 1. The section of the original column before jacketing was 300mmx300mm, the clear span of the column was 1260mm (shear span ratio: 2.1), and the specified concrete strength was 21MPa. Bar arrangements of the main bar and the hoop reinforcement were 8-D13 (p_t=1.13%) and 2-D10 (p_w=0.24%) respectively. All main bars were anchored with the steel plate in the stub. Test column N-0-0 was the original column without retrofitting. The thicknesses of the thin steel plates were 1.6mm and 2.3mm. The amount of FRP was common in all retrofitted columns while the strength of the sheet was not the same. The divided thin plates were welded in the test column SF-2.3W-2 and the thin plates in the other jacketed columns were wrapped by the mortar and FRP sheets without welding in the other retrofitted test columns. Steel plates wrapped by the FRP sheets and the epoxy resin acted as a form of grout mortar. Details of the test columns are shown in Figure 1.

Table 1. List of test columns

Test Column	Section		Steel Thickness (mm)	FRP Sheet		Grout Mortar Thickness (mm)	Note
	Before (mm)	After (mm)		Strength (tonf/m)	Number		
N-0-0	300 × 300	—	—	—	—	—	—
SF-1.6-2		340 × 340	1.6	90	2	20	—
SF-1.6-1				180	1		—
SF-2.3-2			2.3	90	2		—
SF-2.3W-2				90	2		Welding

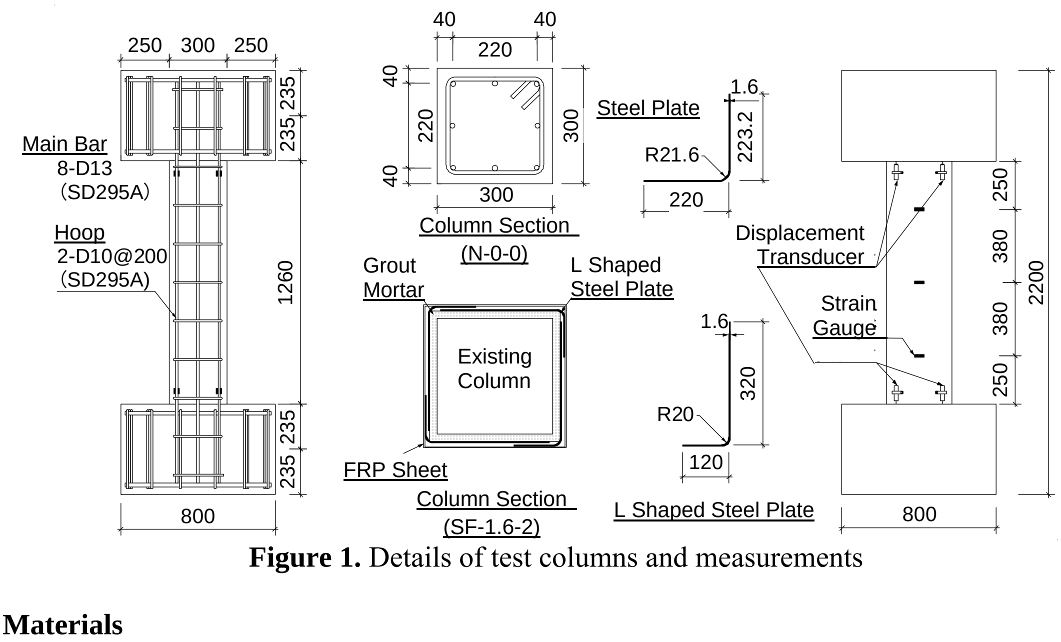

Figure 1. Details of test columns and measurements

2.2. Materials

The mix properties of concrete of 21MPa are shown in Table 2. The water cement ratio of the concrete was 67% and the compressive strength of the concrete and grout mortar measured 28 days after casting was 23.5MPa and 54.9MPa respectively. The test columns and the test cylinder were cured in the air. The compressive strengths of the concrete were approximate to the specified strength. Yield strength of the main bar D13 and the hoop reinforcement D10 were 370MPa and 368MPa,

Table 2. Mix properties of concrete

Specific Strength	W/ C (%)	s/g (%)	Slump (mm)	Air (%)	Unit (kg/m^3)				
					C	W	sand	gravel	Additive
Fc21	67	48	18	3.5	288	194	852	933	2.88

Table 3. Mechanical properties of concrete and grout mortar

Material	Curing	Compressive Strength [N/mm^2]	Tensile Strength [N/mm^2]	Young's Modulus [kN/mm^2]
Concrete	Air	23.5	2.2	25.3
Grout Mortar	Air	54.9	4.4	20.5

Table 4. Mechanical properties of steel and FRP

Material	Diameter, Thickness (mm)	Yield Strength [N/mm^2]	Tensile Strength [N/mm^2]	Young's Modulus [kN/mm^2]
Main Bar	13	370	518	186
Hoop	10	368	520	193
Steel Plate	1.6	283	355	202
	2.3	307	384	208
FRP Sheet	0.428	—	2020	119

respectively. Tensile strength of the polyarylate fiber was 2020MPa more than five times the strength of steel.

2.3. Loading and Measurements

The test setup was designed to subject the test column to lateral load reversals, while the axial load remained a constant ($N=0.2bD\sigma_B$). The top stub was fixed to the L shaped steel beam and the bottom stub was fixed to the reaction floor with high tension bolts. To ensure that the top and bottom stubs remained parallel during reversal loadings, the pantograph system was used. The test setup is shown in Figure 2. The electrical instruments used to measure displacements and the strain gauges used to measure strains of the reinforcing bars were mounted on the columns. The strains of the steel plates and the FRP sheet were also measured with the strain gauges. The lateral and vertical loads were measured by the load cells instrumented between the jacks and the loading beam. Lateral load was applied by the horizontal jack under displacement control.

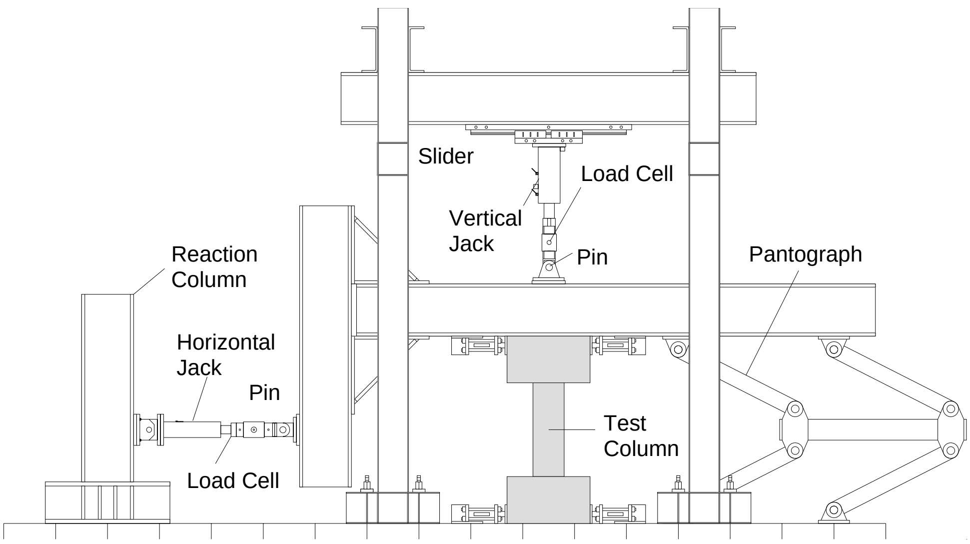

Figure 2. Test apparatus

3. TEST RESULTS

3.1. Crack patterns

Typical crack patterns are illustrated in Photo 1. In the test column without jacketing N-0-0, flexural cracks occurred between the column and the stub at drift angle R=/1400rad. After the flexural cracks progressed, shear cracks occurred in the end area of which length was D (D: column depth) at the drift angle R=1/200rad. Splitting of the cover concrete at both ends occurred at drift angle R=1/100rad, and the maximum strength was measured at the drift angle R=1/66rad. After the maximum strength was reached, crushing of concrete at both ends of the column progressed while the strength decreased. At the final stage, buckling of the main bars was observed. In the jacketed columns the flexural cracks at both ends of the columns were observed throughout the tests. The width of the flexural cracks increased when the lateral displacement increased. It was impossible to observe the crack patterns of the area jacketed by the retrofitting materials. The crack patterns were inspected after the jacketing materials were removed at the end of loading. Neither shear cracks nor splitting of the concrete cover were observed in the mid area of the columns. The columns were not damaged because the column sections were confined by the jacketing.

N-0-0（R=1/33rad.） SF-1.6-2(R=1/8.4rad.)

Photo 1. Crack patterns of concrete columns

3.2. Shear force-drift angle response

Shear force-drift angle hysteretic responses of the test columns are shown in Figure 3. Broken lines and solid lines show the calculated values obtained by Eqn. (3.1) and (3.2) respectively. M_u is the flexural strength, assuming the yielding of the main bars, and Q_{su} is the shear strength in the Standard for Seismic Evaluation of Existing Reinforced Concrete Building. The critical drift angle of 80% of the maximum strength was inserted into the figures.

$$M_u = 0.8a_t \cdot \sigma_y \cdot D + 0.5N \cdot D\left(1 - \frac{N}{b \cdot D \cdot F_c}\right) \tag{3.1}$$

$$Q_{su} = \left\{\frac{0.053 \cdot k_p (18 + \sigma_B)}{M/Qd + 0.12} + 0.85\sqrt{p_w \cdot \sigma_{wy}} + 0.1\sigma_0\right\} b \cdot j \tag{3.2}$$

a_t: Sectional area of main bar (mm^2) b : Column width (mm) D : Column depth (mm)
d : Effective depth of column (mm) F_c : Specified concrete strength (N/mm^2)
j : Internal lever arm (mm) N : Axial force (N) M/Q : Shear span p_t : Ratio of main bar (%)
p_w : Ratio of hoop reinforcement σ_0 : Axial load level (N/mm^2) σ_B : Concrete strength (N/mm^2)
σ_y: Yield strength of main bar (N/mm^2) σ_{wy} : Yield strength of hoop reinforcement (N/mm^2)

In the test column without jacketing, the main bars yielded at the drift angle R=1/100rad. The maximum strength was recorded approaching the drift angle R=1/66rad. After the maximum strength, the shear strength decreased rapidly. The critical drift angle was R=1/48rad, and the vertical load could not be supported when the drift angle reached R=1/25rad. The maximum shear strength can be predicted by Eqn. (3.2). The test columns jacketed by the mortar, steel plate and FRP sheet had similar hysteresis loops that showed significant ductile behaviours. The hysteresis loops were slightly pinched at the origin due to the bond deterioration in the column or the stubs. The maximum strengths were greater than the strength calculated by Eq. (3.1). After the maximum strength was reached, the shear strength did not decrease while the deflection angle became a very large R=1/10rad. The lateral loadings were stopped due to the limit of the loading systems. The thickness of the steel plate and the number of FRP sheets did not influence the shear force-drift angle response.

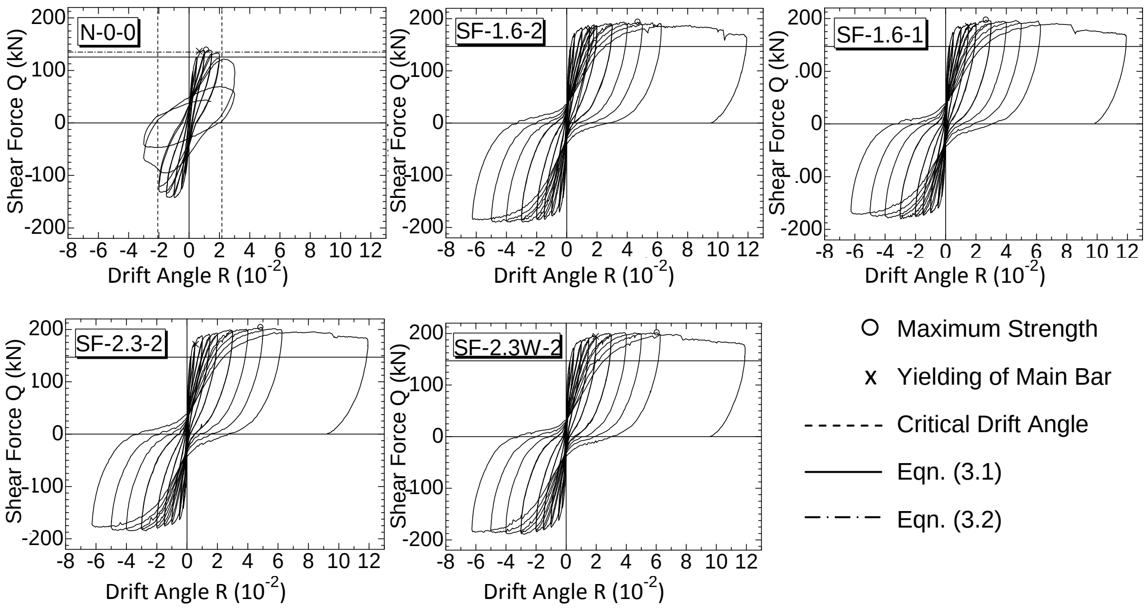

Figure 3. Shear force-drift angle

4. DISCUSSIONS

4.1 Maximum strength

The observed maximum strengths of all the test columns are summarized in Table 4. Flexural strengths obtained theoretically by the two equations are shown in the same table. Equation (3.1) mentioned in the previous section was the simplest one, assuming yielding of the main bars. Ultimate flexural strength M_u was obtained by Eqn. (4.1) considering the equilibrium of the force in the column section as shown in Figure 4. x_n in Eqn.(4.1) is the length of the neutral axis. The concrete strength of the stress block was the average of both the concrete strength and the mortar strength. The maximum strength of the column without jacketing can be predicted by Eqn. (3.1) and Eqn. (4.1) as shown in Table 4, while the test column without jacketing was originally designed to be the flexural failure type. For the column with jacketing the calculated flexural strength by Eqn. (3.1) was 1.23~1.30 times the observed maximum strength.

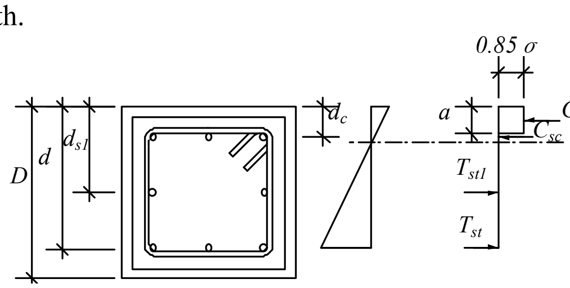

Figure 4. Dimensions of column section

Table 4. Maximum strength

Test Column	Exp. [kN]	Flexural				Shear			
		Eqn.(3.1)		Eqn.(4.1)		Eqn.(4.2)		Eqn.(4.2)	
		Cal.1 [kN]	Exp./Cal.1	Cal.2 [kN]	Exp./Cal.2	Cal.3 [kN]	Exp./Cal.3	Cal.4 [kN]	Exp./Cal.4
N-0-0	139	134	1.04	134	1.04	165	0.84	—	—
SF-1.6-2	193	157	1.23	172	1.13	266	0.73	222	0.87
SF-1.6-1	197		1.26		1.15		0.74	221	0.89
SF-2.3-2	204		1.30		1.19		0.77	222	0.92
SF-2.3W-2	201		1.28		1.18		0.76	254	0.79

$$M_u - 0.5N \cdot D = T_{st} \cdot d + T_{st1} \cdot d_{s1} - C_{sc} \cdot d_c - C_c \cdot \frac{a}{2} \tag{4.1}$$

$$a = \beta_1 \cdot x_n \quad (\beta_1 = 0.85)$$

The strength calculated by Eqn. (4.1) were 1.13~1.19 times of the observed maximum strength. Considering the mortar strength and the main bar at the middle level of the section the calculated values were slightly improved. Equation (4.2) was obtained by truss and arch theory as per the Architectural Institute of Japan's ultimate strength concept. The reduction factor for concrete strength ν was recommended as 0.75 in this concept because the concrete strength in the arch mechanism decreased due to the occurrence of the diagonal shear cracks. However, for the test column with jacketing in this paper, ν was assumed to be 1 according to the result that the shear cracks did not occur in the columns, as shown in Photo 1. The calculated values were overestimated regardless of the strengthening in the test columns. In particular, the observed values of the column with jacketing were approximately 75% of the calculated values.

$$V_A = b \cdot j_t \cdot p_w \cdot \sigma_{wy} \cdot \cot\phi + (1-\beta)\nu \cdot \sigma_B \cdot \frac{bD}{2} \cdot \tan\theta \tag{4.2}$$

$$\beta = \frac{\left(1+\cot^2\phi\right) \cdot p_w \cdot \sigma_{wy}}{\nu \cdot \sigma_B}$$

ν : Reduction factor of concrete strength (ν =1)

As shear cracks did not occur in the test columns with jacketing, it is considered that the hoop reinforcement did not contribute to the truss mechanism. Therefore, ignoring the resistance of the truss mechanism in the truss and arch theory, the arch mechanism is only considered to estimate the maximum strength. The arch mechanism is shown in Fig.5.

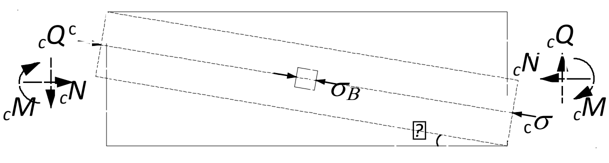

Figure 5. Arch mechanism

$$\sigma_B' = K\sigma_B \qquad K = 1 + \frac{p_r \sigma_{ry}}{\sigma_B} \tag{4.3}$$

$p_r \cdot \sigma_{ry} = p_w \cdot \sigma_{wy} + p_s \cdot \sigma_{sd} + p_f \cdot \sigma_{fd}$

$p_w \cdot \sigma_{wy}$: reinforcement of hoop

$p_f \cdot \sigma_{fd}$: reinforcement of FRP

$p_s \cdot \sigma_{sd}$: reinforcement of steel plate

Based on Richart's study the effects of confinement on the concrete by the jacketing materials are considered in the concrete strength σ_B' in Eqn. (4.3). The confinement effect of the steel plate was taken into account according to the calculated value of the test column SF-2.3W-2, where the divided steel plates were welded. The calculated values Cal.4 by the arch mechanism are shown on the right side of Table 4. The calculated values were close to the observed values, although these values were slightly overestimated.

5. CONCLUSIONS

Based on the test results it was shown that:

1) The proposed retrofitting method could significantly improve the seismic performance of existing RC columns.

2) Neither the number of FRP sheets or steel plates, nor welding of the plates affected the improved performance in the retrofitted columns.

3) It was found that the increased concrete strength (due to confinement by the retrofitting materials) resisted the compression failure of the extreme fiber of the column section.

4) Further inspection to predict the maximum strength of the retrofitted columns using the proposed method is needed.

AKCNOWLEDGEMENT

Part of this research has been supported by the *Japan Ministry of Education, Culture, Sports, Science and Technology* under Grant-in-aid No.21360268. The authors would like to thank the staff and graduate students of the *Structural Earthquake Engineering Lab. of Hiroshima University*.

REFERENCES

Yoshinori Itoh, Eiji Makitani and Eiji Sawazaki; Seismic Strengthening Effect of Low Strength Concrete R/C Columns Retrofitted by Various Methods, *Journal of Structural and Construction Engineering*, Number 613, March, 2007

The Japan Building Disaster Prevention Association: *Seismic Evaluation Standard for Existing Reinforced Concrete Structure*, 2001.

Architectural Institute of Japan: *Design Guidelines for Earthquake Resistant Reinforced Concrete Buildings Based on Ultimate Strength Concept*, 1990.

Richart, F. E. , et al :A Study of the Failure of Concrete under Combined Compressive Stress, *Bulletin No.*185, *University of Illinois Engineering Experiment Station*, Urbana, Nov., 1928